ON THE MEASUREMENT OF SHEAR ELASTIC MODULI AND VISCOSITIES OF ERYTHROCYTE PLASMA MEMBRANES BY TRANSIENT DEFORMATION IN HIGH FREQUENCY ELECTRIC FIELDS

H. ENGELHARDT AND E. SACKMANN
Physik Department (Biophysics Group), Technische Universität München, D 8046 Garching, Federal Republic of Germany

ABSTRACT We present a new method to measure the shear elastic moduli and viscosities of erythrocyte membranes which is based on the fixation and transient deformation of cells in a high-frequency electric field. A frequency domain of constant force (arising by Maxwell Wagner polarization) is selected to minimize dissipative effects. The electric force is thus calculated by electrostatic principles by considering the cell as a conducting body in a dielectric fluid and neglecting membrane polarization effects. The elongation A of the cells perpendicular to their rotational axis exhibits a linear regime (A proportional to Maxwell tension or to square of the electric field E^2) at small, and a nonlinear regime (A proportional to square root of Maxwell tension or to the electric field E) at large extensions with a cross-over at $A \approx 0.5$ μm. The nonlinearity leads to amplitude-dependent response times and to differences of the viscoelastic response and relaxation functions. The cells exhibit pronounced yet completely reversible tip formations at large extensions. Absolute values of the shear elastic modulus, μ, and membrane viscosity, η, are determined by assuming that field-induced stretching of the biconcave cell may be approximately described in terms of a sphere to ellipsoid deformation. The (nonlinear) elongation-*vs.*-force relationship calculated by the elastic theory of shells agress well with the experimentally observed curves and the values of $\mu = 6.1 \times 10^{-6}$ N/m and $\eta = 3.4 \times 10^{-7}$ Ns/m are in good agreement with the micropipette results of Evans and co-workers. The effect of physical, biochemical, and disease-induced structural changes on the viscoelastic parameters is studied. The variability of μ and η of a cell population of a healthy donor is $\pm 45\%$, which is mainly due to differences in the cell age. The average μ value of cells of different healthy donors scatters by $\pm 18\%$. Osmotic deflation of the cell leads to a fivefold increase of μ and 10-fold increase of η at 500 mosm. The shear modulus μ increases with temperature showing that the cytoskeleton does not behave as a network of entropy elastic springs. Elliptic cells of patients suffering from elliptocytosis of the Leach phenotype exhibit a threefold larger value of μ than normal discocytes of control donors. Cross-linking of the spectrin by the divalent S–H agents diamide (1 mM, 15 min incubation) leads to an eightfold increase of μ whereas η is essentially constant. The effect of diamide is reversed after treatment with S–S bond splitting agents.

INTRODUCTION

Precision measurements of viscoelastic parameters of cell plasma membranes of erythrocytes are important for two reasons. First, they are expected to give insight into the microscopic structure of the membranes, in particular concerning the coupling of the spectrin/actin network to the lipid/protein bilayer. Second, they provide a means to characterize the physiological state of the membrane and its changes caused by diseases, metabolic defects, or application of drugs in a quantitative way. Most efforts of elasticity measurements concentrate on erythrocytes because the cytoskeleton forms a thin layer beneath the inner monolayer of the membrane so that the cytoplasm is expected to behave as a liquid.

To evaluate the mechanical properties of membranes in terms of the major elastic contributions, bending stiffness (or flexural rigidity), shear rigidity, and lateral compressibility, it is necessary to apply a variety of techniques which differ in degree of perturbation.

With the familiar micropipette technique (Hochmut et al., 1979) a large range of forces may be applied so as to enable the direct measurement of both the shear and compression elastic moduli (Evans, 1983). Towards small forces the technique is limited by the resolution of suction pressure and the effect of bending rigidity of the cell membrane. Another strong perturbation technique is cell poking (Petersen et al., 1982). Intermediate forces are applied in the cases of the rheological techniques (Fischer et al., 1978*b*; Bessis et al., 1975). However, a quantitative determination of shear elastic moduli has not been achieved yet with the latter technique. The nonperturbing

flicker spectroscopy (Brochard and Lennon, 1975; Fricke and Sackmann, 1986; Zilker et al., 1987) involving deformation energies of the order of kT enables precise measurements of the bending stiffness alone.

The main purpose of the present work is to show that the previously introduced (weak perturbation) technique (Engelhardt et al., 1984) based on the transient deformation of cells in inhomogeneous high-frequency (HF) electric fields allows quantitative measurements of the shear elastic modulus and viscosity of cell plasma membranes. Concerning the quantitative evaluation, one drawback is that the force acts in a direction perpendicular to the axis of rotation so that the deformed cellular shell lacks rotational symmetry. A rigorous calculation of the stress-strain relationship is not possible. This problem is partly overcome by application of a fast image processing system which enables precise measurements of very small deformations ($\geq$500 Å). Absolute values of the shear elastic modulus are thus obtained by comparison of the experimental data with a treatable model, namely the deformation of a spherical into an ellipsoidal shell.

The present technique allows precise and sensitive measurements of relative values of the viscoelastic parameters μ and η of the erythrocytes or other cells. These parameters may in addition be determined as a function of the deformation of the cells by increasing the electric field in a stepwise manner.

In the application part we study changes of the viscoelastic parameters of erythrocyte membranes induced (*a*) by physical manipulation of the membrane structure (e.g., osmotic swelling and temperature variations), (*b*) by biochemical gelation of spectrin via SH cross-linking agents, and (*c*) by membrane defects originating in diseases.

EXPERIMENTAL BASIS OF THE METHOD

Principle of the Method and Measuring Procedure

Fig. 1 shows a schematic view of the experimental set-up and the measuring chamber used for the present experiments. The basic idea is to fix the cell at one of the electrodes by a small bias electric field and to stretch (and relax) it transiently by increasing (and decreasing) the field strength. The elastic constant is obtained by evaluation of the elongation, *A*, as a function of the electric (Maxwell) tension. The membrane viscosity is obtained from the response times of the cellular deformation after field jumps. The essential progress compared with previous preliminary experiments (Engelhardt et al., 1984; Sackmann et al., 1984) is the precise measurement of the extension by a fast image-processing system that allows measurements of deformation amplitudes as small as 50 nm in the time scale of some 10 ms without time averaging. It should be noted that by fixing the cell its Brownian motion is suppressed, which is essential for the precision measurements of cellular elongation. Moreover by using wedge-shaped electrodes, clear images of the cells are obtained, whereas these are optically distorted in the case of circular electrodes such as wires.

Three modes of operation are applied: (*a*) a continuous deformation and release procedure, (*b*) a field jump method, and (*c*) a stepwise deformation and release procedure.

In the *a* case the voltage is linearly increased and decreased by application of a triangular pulse. The rise time is large (4 s) compared with the response time of the cell (≈0.1 s). The deformation amplitude is recorded as a function of the field strength. Fig. 2 shows images of a deformed cell as a function of the field strength, and the top of Fig. 3 exhibits a record of the deformation, *A*, after application of a triangular electric pulse.

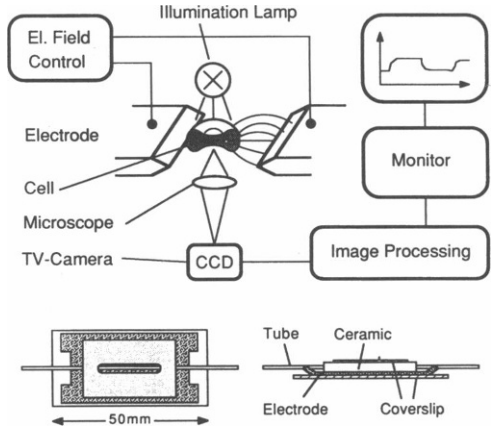

FIGURE 1 (*Top*) Schematic view of measuring system consisting of measuring chamber, microscope, electric field control, CCD-television camera, and fast image processing system. Note that the cell is attached to one of the electrodes in such a way that its rotational axis is perpendicular to the plane of the electrodes. (*Bottom*) Birdsview (*left*) and sideview (*right*) of the measuring chamber as described in text.

In the *b* case a rectangular pulse is applied with a rise time small compared with the response time of the cellular deformation. This corresponds to the classical creep-after-sudden-stress experiment of viscoelasticity and has been applied previously (Engelhardt et al., 1984). A typical response and relaxation curve is presented in Fig. 6.

In procedure *c* the electric field is first increased in a stepwise manner with equal increments in *E* to a maximum value E_{max}, and the response function is recorded for each step. Thereafter the voltage is decreased in a reverse way. A typical response curve is shown in Fig. 3, *bottom*. Note that the elongations A_i of each step i increase with increasing elongation, whereas the relaxation time decreases with increasing elongation.

Measuring Chamber

Fig. 1 shows a schematic view of a measuring chamber which allows perfusion of the cells during the measurement. It consists of two halves of a razor blade sandwiched between a cover glass 50 × 25 × 0.14 mm³ and a glass-ceramic body of 30 × 20 × 3 mm³ outer dimensions and an opening of 20 × 5 × 3 mm³. The body is covered by a cover glass of 25 × 25 × 0.14 mm³. The system is glued together with nail varnish and the chamber may be perfused via two tubes through the ceramic body. To avoid the escape of ions from the glass-ceramic body it is covered by varnish. Before each measurement the chamber is washed by pumping distilled water through it for at least 2 h. Because the erythrocytes tend to stick to the electrodes after some time the chamber is taken apart and the pieces are washed carefully in aceton after about every 20th measurement. For temperature control the measuring cell is positioned in a sample holder made of massive copper, which is in contact with two Peltier elements. In separate experiments we measured the voltage-current curves of the measuring chamber to determine the electrode polarization. From these experiments it follows that it is of the order of some millivolts in the frequency range used here and can thus be ignored.

Microscope

The cells are observed and measured with a modified Zeiss Axiomat inverted microscope (objective: Planapo 50×/0.95 Pol). The light source is a 100-W halogen lamp. To minimize photochemical decompositions, we

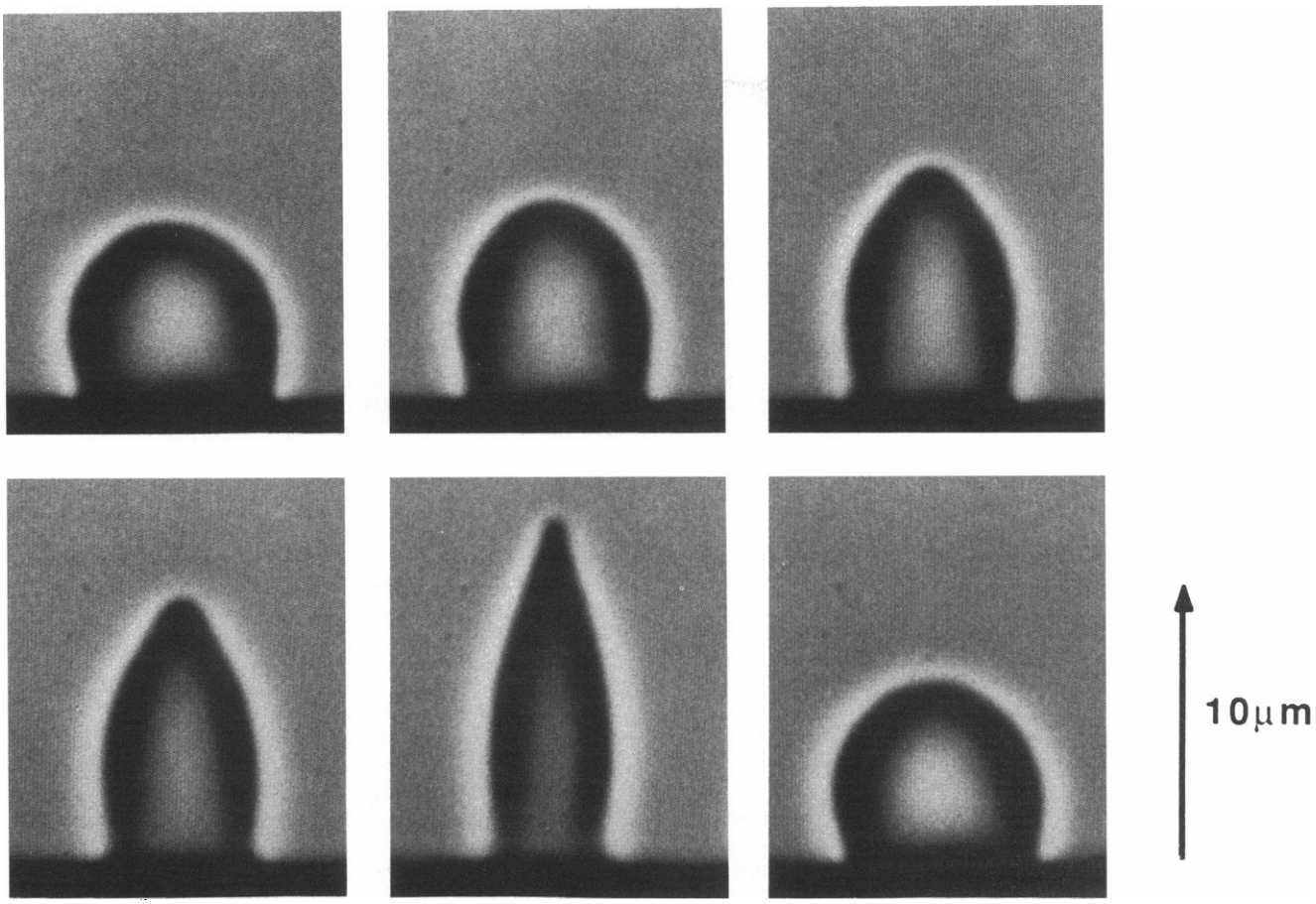

FIGURE 2 A single red cell is shown in different states of deformation caused by a high-frequence electric field. The corresponding electric field strengths are from left to right 5, 20, 35, 50, 150, 0 kV/m, respectively. Note that even elongations >6 μm are reversible (see last micrograph which is obtained after removing the electic field). Another interesting observation is the tip formation at elongations >3 μm.

removed short wavelength light by a UG 540 filter (3 mm; Schott Glass Technologies Inc., Duryea, PA). Heating of the chamber is prevented by filtering out infrared light with a Schott KG 1 filter (3 mm).

Electric Field Control

For the high-frequency electric field generation and amplitude modulation, a Hewlett-Packard function generator (HP 8112) is used. The generator is controlled by an Apple II computer via an IEC-bus which simplifies the application of various measuring programs such as field jumps, triangular pulses, or frequency scans (cf. Fig. 4). Voltage, current, and temperature are measured and recorded during each measurement.

Image Processing

Hardware. For measurement, images of the cells are taken with a CCD-camera (type SM72 operating with an interframe transfer chip; Aqua-TV, Kempten, FRG), in such a way that a section of $5 \times 5\ \mu m^2$ is projected onto the light-sensitive area corresponding to a 50,000-fold enlargement on the monitor (cf. Fig. 5). The resolution of the image storage system is 18 nm per pixel. The resolution of the deformation amplitude measurement is thus limited by the fluctuation of the contour owing to Brownian motions (flickering) of the cell surface, which exhibits amplitudes of ~40 nm.

The signal of the charge-coupled device camera (CIRR norm) is either directly fed to the image processing system built in this laboratory (by H. Engelhardt) or stored in a UMATIC video recorder (Sony VO 5800 PS). The TV signal is digitized on line with 10 MHz and 8-bit resolution (256 grey levels). This yields 50 digitized frames per second with 512*256 pixels (or 25 frames per second with 512*512 pixels). The processed images are displayed on a TV-monitor after digital to analog conversion. The whole system is controlled by a computer (type SAM; KWS, Karlsruhe, FRG) equipped with an MC 68000 processor.

Software. To measure the transient deformation amplitude, a narrow stripe of the image (which is marked by a dashed line in Fig. 5) is further processed. For that purpose the data of this section are transferred to the computer memory every 20 ms. After finishing the measurement these stripes are put side by side according to their chronological order. This way a new image is formed where the ordinate is the spatial axis (parallel to *E*-field direction) and the abscissa is the time axis (cf. Fig. 5, *right*).

the transient position of the membrane is determined with a resolution of 18 nm (one pixel) by the following cross-correlation procedure. The intensity pattern along one of the stripes (cf. Fig. 5) is taken as reference pattern $M(x,t_0)$. $M(x,t_0)$ is cross-correlated with each other intensity pattern $I(x)$ of each stripe.

$$K(x) = \sum_u I(x + u) * M(u) \qquad (1)$$

Thus the function $K(x)$ has a maximum where the reference intensity pattern $M(u,t_0)$ and the intensity pattern in each stripe $I(x)$ match best.The location of the maxima of $K(x)$ in each stripe gives the shift of the membrane position due to deformation. For further improvement of the signal-to-noise ratio the variations in the sensitivity of the photodiodes of the CCD camera are corrected. Typical response curves detected by this procedure are given in Fig. 6 or Fig. 10.

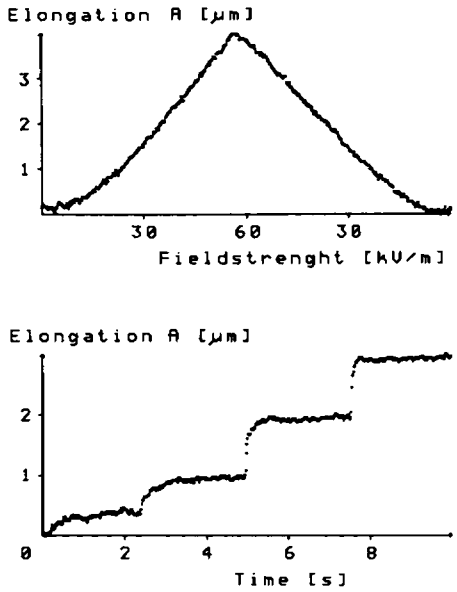

FIGURE 3 (*Top*) Typical elongation-vs.-field strength dependence of an erythrocyte. Here the electric field strength is first linearly increased with time up to a maximal value (within 5 s) and then linearly decreased to zero field strength. For small elongations a parabolic and for larger elongations a linear relation between the elongation and the field strength is observed. (*Bottom*) In the step operational mode the field strength is increased from zero field in four steps (12 kV/m each step) up to 48 kV/m and the response of the cell is measured. The cell membrane viscosity determines the time needed to reach the new equilibrium shape. Note that the relaxation times depend on the deformation amplitude. This is due to nonlinear effects caused by the geometry of the cell. Plastic deformation is not observed.

To determine the response times of the creep and relaxation functions, we approximated these by exponential functions with one or two relaxation times according to

$$A(t) = A_0 + B \exp(t/\tau_B) + C \exp(t/\tau_C). \quad (2)$$

An example is given in Fig. 6 which shows that good agreement is obtained with a double-exponential fit. Note that the temporal fluctuations in the amplitude in Fig. 6 are due to the flickering of the membrane which exhibits amplitudes of the order of 40 nm. This demonstrates the sensitivity of the present technique.

Materials and Cell Preparations

All chemicals used: diamide (diazindicarboxylic acid-bis-dimethylamid); jodoacetate; CDE (cystindimethylester), mannitol, D-glucose, and $CaCl_2$ are commercial products. The S-ACD-buffer is composed of 106 mM NaCl, 11 mM Na_3-citrate, 25 mM glucose, 100 μM adenin, 100 μM inosin, 3 mM $CaCl_2$, 5 mM KCl. In addition it contains 5 vol % fetal calf serum (Boehringer Mannheim GmbH, Mannheim, FRG), 1 vol % seromed No. K2731 vitamine solution (Biochrom Kg, Berlin, FRG), 1 vol % seromed No. A2213 penicillin-streptomycin solution (Biochtrom KG, Berlin, FRG), and 0.2 wt % albumin (BSA; Serva Fine Biochemicals Inc., Garden City Park, NY). The pH is adjusted by citric acid to pH 7.4 and the osmolarity is 300 mosm. The measuring solution contains 250 mM mannitol, 30 mM glucose, and 1 mM $CaCl_2$.

Preparation of Cells

Cells from patients suffering from elliptocytosis were kindly provided by Dr. M. J. A. Tanner (Department of Chemistry, Medical School, Bristol, UK). They were shipped together with control cells of healthy donors. The measurements of these cells were performed 6 d after bleeding.

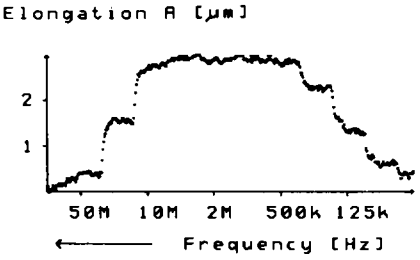

FIGURE 4 The force acting on the cell membrane due to the ac electric field has a characteristic frequency dependency. Outside the plateaulike region from 500 kHz to 5 MHz the force is strongly frequency dependent. The curve is obtained by decreasing the frequency of the electric field every second in steps (52 MHz, 30 MHz, 10 MHz, 5 MHz, 2 MHz, 1 MHz, 500 kHz, 250 kHz, 125 kHz, 62 kHz, 31 kHz) while the amplitude is kept constant.

Normal cells are taken from healthy volunteer donors of this laboratory. Depending on the amount of cells needed, blood is drawn from the arm vein or the fingertip. The blood is first diluted with ACD buffer by a factor of four. It is then washed by centrifugation at 1,000 *g* for 3 min and the supernatant and the buffy coat are removed. Then the cells are diluted 100-fold with ACD buffer. In the presence of serum the cells can be stored for ~1 wk without remarkable shape changes. However, the cells (except the elliptocytotic) are always measured at the day of bleeding.

The density separation of cells occurs by centrifugation of the freshly drawn blood (diluted with fourfold amount of ACD buffer) at 12,000 *g* for 15 min (Nash et al., 1983). The upper 10% and lower 10% of the cells are then used for measurement.

To generate a force by Maxwell-Wagner polarization, the conductivities of the outer medium σ_0 and the cytoplasm σ_i must differ typically by an order of magnitude. Therefore the cell suspensions are diluted by a factor of 100 with the measuring solution to adjust the conductivity of the outer medium to a value of $\sigma_0 = 0.02\ \Omega^{-1}m^{-1}$. In the measuring solution the cells do not exhibit changes of the shape or the elastic constant for ~15 min, which is the upper limit of the measuring time. This lifetime is only achieved by washing the chamber with serum and/or with vesicle suspension before the cells are filled in for the first time. This procedure must probably reduces the exit of ions from the razor blades.

THEORETICAL BASIS OF THE METHOD

Model of Electric Force Generation

As discussed previously (Engelhardt et al., 1984, Sackmann et al., 1984) the force is generated by Maxwell-Wagner polarization of the cell in a frequency domain where the cytoplasm is conductive but not the outside medium. The calculation of the electric force is very complicated if dissipative processes become essential (Sauer, 1983). This is certainly the case if the forces are frequency dependent. Therefore all experiments are performed in a frequency domain where the force is constant and dissipative processes such as those associated with cell rotation (Zimmermann et al., 1980; Saito et al., 1966) are small. For that purpose the conductivity of the outside medium is kept small compared with that of the cytoplasm so that the force may be calculated by means of the familiar electrostatic principles by treating the cell as a conducting body in a dielectric fluid. Notwithstanding

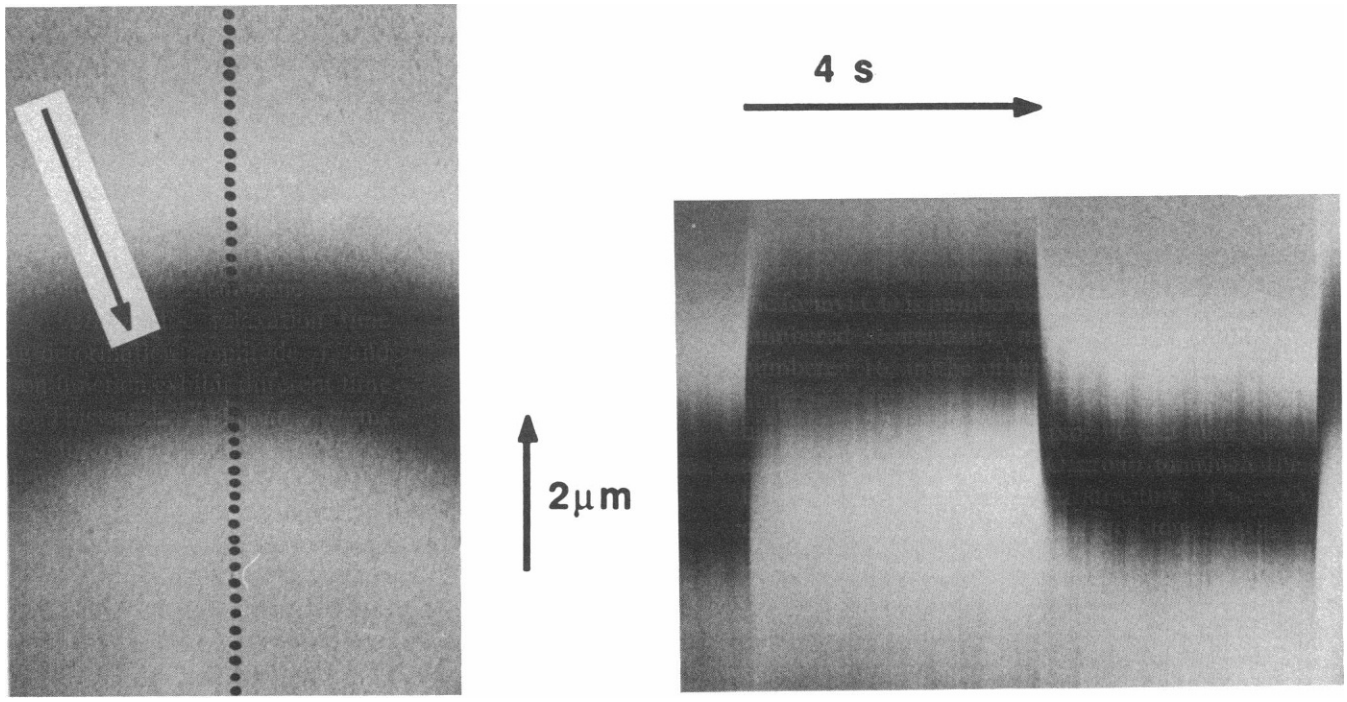

FIGURE 5 (*Left*) Image of a small section of the cell envelope (*arrow*) as seen on monitor during the measurement. For further analysis the intensity distribution along the vertical slice marked by dashed lines is stored on-line in the image processing system every 20 ms. (*Right*) Record of elongation and relaxation of the cell. The electric field is switched every 4 s between 20 and 40 kV/m. The image is formed by rearranging the intensity distribution along the vertical slice marked by the dashed line which is sampled every 20 ms in such a way that the time axis runs from left to right side. The displacement of the cell border is obtained by image processing (see text) resulting in a graph such as shown in Fig. 6. By this common procedure for analysis of the shear modulus and the membrane viscosity the elongation of a cell can be measured to an accuracy of ≈50 nm.

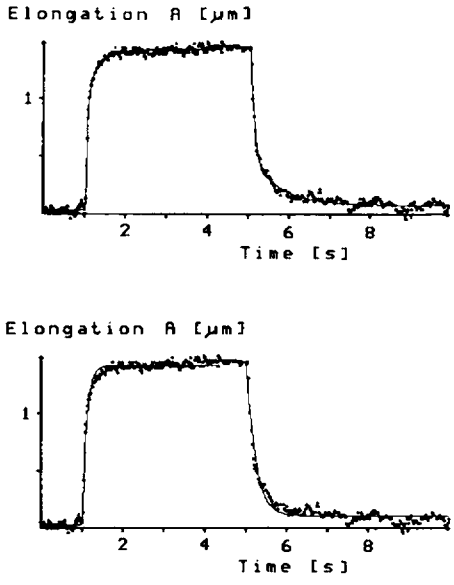

FIGURE 6 Transient elongation of a cell after application of an electric pulse. The high frequency electric field is switched between 20 and 40 kV/m every 4 s. Response curves are fitted very well by double exponential fits (*top curve*) but not sufficiently well with a single exponential fit (*bottom curve*). The membrane viscosity is obtained from the time the cell needs to reach a new equilibrium state and the shear elastic modulus obtained from the maximum elongation.

these simplifications we introduced the following approximations to avoid tedious numerical calculations. (*a*) The cell geometry is reduced to a sphere which is deformed into an ellipsoid with the long axis parallel to the electric field direction. (*b*) The cell is considered to be in a homogeneous external electric field E_∞, where E_∞ is taken as the field strength in the measuring chamber at a distance of 4 μm from the edge of the electrode. (*c*) The cytoplasm, the extracellular medium, and the membrane are considered isotropic, and polarization effects of the membrane are neglected. (*d*) The variation of the force with the elongation of the cell is neglected.

The above approximations will be justified in the following and it will be shown that the Maxwell tension acting perpendicular to the cellular shell is (in Pa V^{-2})

$$\Pi = 0.375\, U_0^2 \cos^2\Theta, \tag{3a}$$

where U_0 is the peak voltage of the HF-field and Θ the polar angle defined in Fig. 8. Integration over the half sphere leads to the total force (in $N \cdot V^{-2}$)

$$f \approx 7 \cdot 10^{-12} U_0^2. \tag{3b}$$

Field Strength Acting on the Cell

The electric field strength at the position of the cell is approximately calculated by solving the Laplace equation

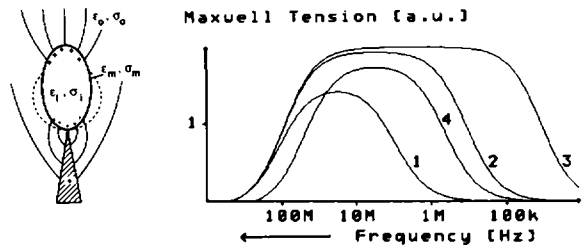

FIGURE 7 (*Left*) Schematic view of a cell in an inhomogeneous electric field showing snapshot of Maxwell-Wagner polarization which arises at interfaces of materials with different conductivities. In the experiment the conductivity of the medium is $\sigma_0 = 0.02\ \Omega^{-1}m^{-1}$ and that of the cytoplasm is $\sigma_i = 0.5\ \Omega^{-1}m^{-1}$. The cell membrane can be regarded as an insulator. The relative dielectric constants of the medium and the cytoplasm are $\epsilon_0 = 80$ and $\epsilon_i = 60$, respectively. These values are used for calculating the force acting on the cell membrane due to the high frequency electric field. (*Right*) Theoretical frequency dependence of the Maxwell tension on a spherical cell membrane due to Maxwell-Wagner polarization showing that the conductivity of the inner medium determines the cutoff at high frequencies, whereas that of the outer medium determines the cutoff at low frequencies. Curve 1 shows the behavior for $\sigma_i = 1\ \Omega^{-1}m^{-1}$ amd $\sigma_0 = 0.1\ \Omega^{-1}m^{-1}$. Curves 2 and 3 show the behavior for lower conductivities of the outer medium, namely $\sigma_0 = 0.01\ ^*\ \Omega^{-1}m^{-1}$ and $\sigma_0 = 0.001\ \Omega^{-1}\ m^{-1}$, respectively, but the same value of σ_i. Curve 4 shows the theoretical frequency dependence for values (see above) used in the present experiment. Note that in the plateau region ($\sigma_0 \ll \sigma_i$) the force on the cell membrane is essentially independent of all structural details of the medium the cytoplasm and the cell membrane. The model reduces to an ideally conducting body in an insulating medium.

for the idealized case of two wedge-shaped electrodes of infinite length which exhibit sharp edges. The corresponding calculations are given in the textbooks (cf., Landau and Lifschitz, 1960, vol. 8, ch. I.3). The essential result is that the field strength in a direction perpendicular to the edges of the electrodes depends rather weakly on the distance, r, from the electrode surface according to

$$E \approx 0.336\ U_0(1/\sqrt{d \cdot r}), \tag{4}$$

where d is the electrode distance ($d = 120\ \mu m$) and U_0 the voltage (in volts). This approximation holds for distances

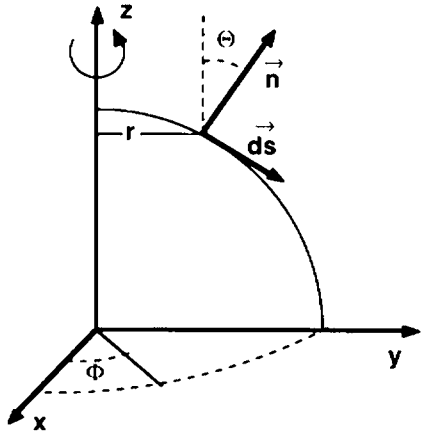

FIGURE 8 Definition of coordinates and parameters characterizing the shell of revolution.

larger than some micrometers. At a distance of $r = 4\ \mu m$ from the electrode surface, that is at the cell center one obtains $E = 15{,}300\ U_0$ in V/m. According to Eq. 3 the square of the field strength (that is the force) decreases from the center to the distal end of the cell by only 10% per micrometer.

Variation of the Electric Force with Degree of Deformation

A further question concerns the variation of the electric force with increasing ellipticity of the cell which could of course also contribute to the nonlinearity of the deformation behavior (cf., Fig. 3, *top*). To the first approximation the electrostatic energy of an ellipsoid in a homogeneous electric field depends linearly on the elongation (Landau and Lifschitz, 1960, Vol. 8, Ch. 4); that is, the variation of the force with elongation is a second order effect. By solving the Laplace equation in ellipsoidal coordinates and by exact calculation of the force as function of the elongation, A, it was shown that for $A < 2\ \mu m$ the force increases only by ~ 10% per micrometer (H. Engelhardt, 1987).

In summary, the slight decrease of the field strength with distance from the electrode surface according to Eq. 4 compensates the increase of the force with elongation of the ellipsoidal shell. Therefore the approximation four made above appears to be well justified.

Frequency Dependence of the Electric Force

The frequency dependence of the dielectric constants ϵ_i and of the conductivities σ_i are negligible (Sackmann et al., 1984) because the Debye relaxation times of the salt solutions are short ($\tau \leq 10^{-7}$ s) compared with the reciprocal frequency. A second origin of the frequency dependence is the boundary condition that the tangential component of both the electric and the magnetic vector of the quasistationary electric field, $E(z,t) = E_\omega \exp\{i\omega t\}$, are continuous at the interfaces of the membrane to the cytoplasm and to the outside medium, respectively (Pohl, 1978). Thus,

$$(\sigma_a + i\omega\epsilon_a)E_a = (\sigma_b + i\omega\epsilon_b)E_b, \tag{5}$$

where a and b denote any of the different media.

According to unpublished calculations (Engelhardt, 1987) the force on the cell with fixed conductivity of the cytoplasm ($\sigma_i = 0.5\ \Omega^{-1}m^{-1}$) is frequency independent over a broad range which depends on the conductivity of the outside medium σ_0. The frequency dependence of the force has been calculated by solving the Laplace equation for a spherical shell and the boundary condition of Eq. 5 by ignoring the electric field inhomogenity. The solutions are given in textbooks such as Landau and Lifschitz (1960). The rather cumbersome equations are solved numerically. Some theoretical curves obtained for different values of the conductivities of the cytoplasm (σ_i and the outside medium

(σ_0) and a nonconductive membrane are plotted in Fig. 7. These can be compared with Fig. 4 where a typical experimentally determined elongation-vs-frequency relationship is shown. The latter is obtained by measuring the deformation amplitude A for a given field strength while the frequency is reduced every second from 50 MHz to 32 kHz in 12 steps. In agreement with the theoretical curve a broad plateau is observed. The conductivities are $\sigma_i = 0.5\ \Omega^{-1}m^{-1}$ and $\sigma_0 = 0.02\ \Omega^{-1}m^{-1}$; that is, the decreases of A at both low and high frequency agree reasonably with the theoretical prediction.

The lower and upper corner frequencies are determined by the breakdown of the conductivities of the outer medium and the cytoplasm, respectively. The lower value agrees most probably with the low dispersion frequency of the Pauly-Schwan theory (cf. Schwan, 1985). A theory of cellular deformation by an electric field was proposed by Bryant and Wolfe (1987). These authors consider also the case of a sphere-to-ellipsoid deformation and therefore introduce an osmotic restoring force. On the other side they treat the case of static field and thus do not account for the Maxwell-Wagner polarization. For that reason the force calculated by this model is frequency independent up to the reciprocal of the time constant for the membrane charging process. Their expression for the electric force agrees with our results in the constant domain.

In the inhomogeneous field, grad (E^2) terms contributing to the force have to considered. However, from the theory of Sauer (1985) we estimate that the force caused by the grad (E^2) terms amounts to ~10% of the force given in Eq. 3b and the additional distortion of the cellular shape caused by the field inhomogenities can thus be ignored in the limit of small deformations considered here.

Elastic Model of Cell Deformation

The basic problem of biomembrane elasticity is the separate determination of the different elastic moduli characterizing the mechanical properties of cellular shells: the bending stiffness, K_c; the lateral compressibility, κ; the surface tension, γ; and the shear elastic modulus, μ (Evans and Skalak, 1980). Because in the present work we deal only with cells of biconcave shape (discocytes) and small deformations (in constant area and volume), contributions of the surface tension and lateral extensions can be ignored. On the other hand, because we consider also deformations that are not small compared with the cell dimensions, nonlinear effects have to be considered. This follows clearly from the experimentally observed transition from a parabolic to a linear regime (cf., Fig. 3).

Because the cells are deformed in a direction perpendicular to the rotational axes so that the cylindrical symmetry is broken, an analytical calculation of the elastic strain as a function of the (Maxwell) stress is not possible. Therefore we assume again that for the range of elongations studied in the present work the deformation can be approximately described in terms of the sphere-to-ellipsoid deformation model under the action of an axisymmetric (electric) field. It is well known from the theory of thin shells (Flügge, 1973; Landau and Lifschitz, 1959, Vol. 7) that for the case of inextensional deformations the bending stresses are small compared with the shear stresses. Thus in the linear regime, the elastic energy associated with pure shear is of the order of $G_{shear} \approx \mu\,\Delta\,(a-b)^2$ and with pure bending $G_{bend} \approx G_{shear}\,\Delta^2/(a+b)^2$ (cf., Flügge, 1973, Ch. 6), where a and b are the principal axes of the ellipsoid and Δ the shell thickness. The former contribution is thus about a factor of 10^{-4} smaller then the latter for the case considered.

For pure shear the deformation of a shell of revolution (cf., Fig. 8) under a force acting everywhere perpendicular to the surface is described by the following equilibrium conditions (Evans and Skalak, 1980; Flügge, 1973, Ch. 2.1)

$$\frac{T_m}{R_m} + \frac{T_\phi}{R_\phi} = P_{el} = P_0 \cos^2\Theta \tag{6}$$

$$\frac{d(T_m r)}{ds} - T_\phi \frac{dr}{ds} = 0, \tag{7}$$

where T_m and T_ϕ are the stresses (in dyn/cm) in directions parallel to the meridian and the circle of latitude, respectively, and R_m and R_ϕ are the principal radii of curvature with respect to these orthonormal coordinates which are given by

$$R_m = \frac{ds}{d\Theta}, \qquad R_\phi = \frac{r}{\sin\Theta}, \qquad \frac{dr}{ds} = \cos\Theta. \tag{8–10}$$

P_{el} is the pressure owing to the Maxwell-Wagner polarization.

Following Evans and Skalak (1980) it is useful to introduce the isotropic stress T_i and the shear stress T_s according to

$$T_s = \frac{T_m - T_\phi}{2}, \qquad T_i = T_m - T_s, \tag{11, 12}$$

and to describe the deformation in terms of the local stretching ratio λ,

$$\lambda = \frac{ds}{ds_0}, \tag{13}$$

where ds_0 is the line element of the undeformed and ds that of the deformed shell. Because the area is constant ($r\,ds = r_0 ds_0$) it follows that

$$r = r_0/\lambda \qquad ds = \lambda\, ds_0. \tag{14, 15}$$

By inserting Eqs. 8–15 into Eqs. 6 and 7 it follows that

$$\frac{d\Theta}{ds_0} = \lambda\left[\frac{P}{T_m} + \frac{\lambda \sin\Theta}{r_0}\left(2\frac{T_s}{T_m} - 1\right)\right] \tag{16}$$

$$\frac{d\lambda}{ds_0} = \frac{1}{r_0}(\lambda\cos\Theta_0 - \lambda^3\cos\Theta). \tag{17}$$

The meridional stress, T_θ, may be eliminated by taking into account that at a given azimutal angle θ the equilibrium condition between the external force and the stress in the z-direction of the electric field is

$$F_z = 2\pi r \sin\Theta\, T_m = 2\pi \int_0^{s_0} r_0 \cos\Theta\, P\, ds_0. \qquad (18)$$

The second equality is a consequence of the condition of constant area. It is derived from

$$dr = \frac{dr_0}{\lambda} - \frac{r_0}{\lambda^2} d\lambda. \qquad (19)$$

Finally Hook's law may be taken into account by the following relation between the shear stress, T_s, and the stretching ratio λ (Evans and Skalak, 1980).

$$T_s = \frac{\mu}{2}(\lambda^2 - \lambda^{-2}) \qquad (20)$$

The differential Eqs. 16 and 17 have been numerically solved with the Runge-Kutta procedure using a shooting technique (Flanders, 1984).

Some results are presented in Fig. 9. On the left side, contours of the shell for increasing Maxwell tensions are presented which show that a spherical shell is deformed into a rotational ellipsoid under the action of the homogeneous electric field. The field dependence of the amplitude, A, of the deformation in the z-direction is plotted on the right side of Fig. 9, for several values of the shear elastic modulus μ. Clearly, the A-vs.-E curves exhibit a parabolic regime for $A < .05$ μm which goes over into a linear regime at large elongations in complete agreement with the experimentally observed curves (cf., Fig. 3). This provides an experimental proof for our assumption that the elongation of the discocyte may be approximately described in terms of the sphere-to-ellipsoid deformation model to determine shear elastic moduli. The shear moduli are obtained by comparing the slopes of experimental and theoretical curves in the linear regime (cf., Fig. 9, *right*, and Fig. 3, *top*).

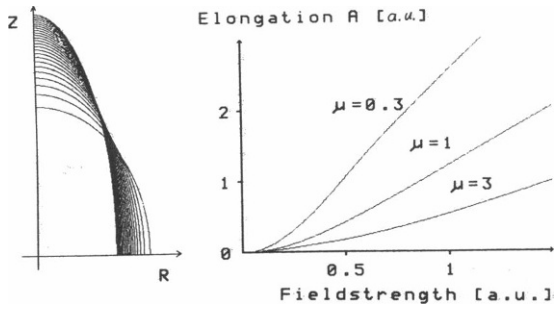

FIGURE 9 (*Left*) Sections (one octant) through long axes of shell of revolution as calculated with Eqs. 16 to 17 for different ratios of the Maxwell tension divided by the shear modulus P/μ (equal steps). (*Right*) Plot of elongation A as a function of field strength for three different values of the shear elastic modulus μ. Arbitrary units are used for all parameters. Very similar to the experimental curves these theoretical function exhibit a parabolic behavior for small deformations and a linear for large ones (cf., Fig. 3). The shear elastic modulus is obtained by comparison of the slopes in the linear regions of the theoretical and the measured curves.

Time Dependencies of Viscoelastic Response

The rise and relaxation times of the viscoelastic response functions are mainly determined by the membrane viscosity. According to Fig. 3, *bottom*, the relaxation time decreases with increasing deformation amplitude A_∞ and the response and relaxation function exhibit different time dependencies for large A_∞. This can be explained in terms of the nonlinearity of the force-elongation curve (force proportional to A_∞^2). This behavior can approximately be described by a nonlinear response equation,

$$\eta \frac{dA}{dt} + \frac{\mu}{R_0} A^2 = \frac{\mu}{R_0} A_\infty^2, \qquad (21)$$

where R_0 is the cell diameter and A_∞ the final amplitude. The solution is of the form,

$$A(t) = A_\infty \frac{c \exp(t/\tau) - 1}{c \exp(t/\tau) + 1}, \qquad (22)$$

where

$$c = \frac{A_\infty + A_0}{A_\infty - A_0}, \qquad \tau = \frac{\eta R_0}{2 f A_\infty}, \qquad (23, 24)$$

and A_0 is the starting amplitude. Clearly Eq. 21 describes our finding that the relaxation time decreases with increasing A_∞ (cf., Fig. 3, *bottom*).

Eq. 22 can be expanded into a sum of exponential functions. As follows from Fig. 6 the experimental curves can be fitted well by a double exponential function according to Eq. 2. In general the fast component accounts for 80% of the amplitude and thus the membrane viscosity is determined from the corresponding relaxation time τ according to

$$\eta = 2\tau\mu A_\infty / R_0. \qquad (25)$$

τ is determined by fitting Eq. 2 to the experimental response or relaxation curve (Marquardt, 1963). It is interesting to note that the relationship $\tau E^2 = \text{const}$ appears to have general validity. It also holds for instance for the orientation of polyelectrolytes or the formation of chains of cells in alternating fields (cf., Schwan, 1985).

APPLICATION OF ELECTRIC FIELD TECHNIQUE TO STUDY CHANGES OF MEMBRANE VISCOELASTIC PARAMETERS CAUSED BY PHYSICAL OR BIOCHEMICAL MODIFICATIONS AND DISEASES

In the following we present some measurements of the shear elastic moduli and membrane viscosities of erythro-

cytes which were undertaken to test whether the present technique is reproducible and sensitive enough to detect subtle changes of the membrane structure as caused by physical and biochemical modifications of the membrane as well as by disease.

Because the prefactors in Eqs. 3 and 4 depend somewhat on the geometry of the measuring chamber, the absolute values of μ and η may vary from one series of measurements to another and they are therefore usually measured relative to control cells. Therefore freshly drawn control cells are measured parallel to each experiment aimed to study the effect of structural changes on μ and η.

To get information about the variability of the viscoelastic parameters of cells of normal donors these are measured for ~50 cells of five donors using the same measuring chamber. Moreover the effect of cell age is examined by measuring old and young cells separated by centrifugation (Pfafferot et al., 1985). The results are summarized in Table I. The average value of the shear modulus of all cells is $\mu = 6.1 \times 10^{-6}$ N/m and the membrane viscosity $\eta = 3.4 \times 10^{-7}$ Ns/m. This is in good agreement with micropipette data (Evans and Skalak, 1980; Hochmut, 1980).

The standard deviation from the average value of μ is ±45% for cells of a single donor preparation, whereas the variability of the average values of μ of the cells of different donors amounts only to ±18%. This suggests that the rather large variation found for cells of one donor is due to their different age. Evidence for this is indeed provided by the finding of Table II according to which the lightest fraction of cells exhibits a considerably smaller shear rigidity and membrane viscosity than the heaviest population. This is in agreement with measurements of the bending elastic modulus by the flicker spectroscopy which show a similar variability of this parameter for a single donor.

The accuracy of the measurement of μ for a single cell is ±4%. Therefore physical or biochemical-induced changes of the cell membranes caused during the measurement and within the lifetime of the cells (15 min) may be detected with high reliability, whereas it is much more difficult to detect differences between the viscoelastic parameters of different donors even if the cells are density separated.

TABLE I
SUMMARY OF VISCOELASTIC PARAMETERS (μ AND η) OF SEVERAL CELLS OF FIVE DIFFERENT DONORS MEASURED AT 24°C

Donor	μ	η	No.
	10^{-6} N/m	*10^{-7} Ns/m*	
1	5.43 ± 50%	3.20 ± 59%	8
2	7.89 ± 61%	3.35 ± 68%	9
3	5.56 ± 39%	3.79 ± 50%	5
4	5.21 ± 36%	2.96 ± 44%	11
5	6.40 ± 38%	3.79 ± 51%	12
Mean	6.1 ± 18%	3.4 ± 11%	

No. is the number of cells measured for each donor.

TABLE II
RESULT OF DENSITY SEPARATION OF CELLS

Fraction	μ	η	No.
	Relative units	*Relative units*	
Upper	1 ± 36%	1 ± 43%	41
Lower	1.82 ± 55%	2.04 ± 67%	38

Viscoelastic parameters of 10% of the lightest and 10% of the heaviest fraction of cells centrifugated at 12,000 g for 15 min.

Physically Induced Structural Changes

In Figs. 10 and 11 we summarize results concerning possible effects of physically induced structural changes of the cell on the viscoelastic parameters of the erythrocytes.

Osmolarity Changes. Fig. 10 shows examples of the effect of osmotic swelling and deflation of the cells on the shear rigidity and creep functions. Both μ and η increase drastically at high osmolarities when the cell deflates but do not change at moderate swelling. Another remarkable effect is shown by the relaxation time. Whereas under normal conditions the response time τ decreases with increasing amplitude as predicted by Eq. 24 (Fig. 3, *bottom*), a reverse behavior is observed at 500 mosm. In the deflated state τ increases by about a factor of two if the amplitude as doubled as follows from Fig. 10, *bottom*.

At present we do not have an explanation for the above effects, which could have several origins: (*a*) the influence of the cytoplasmic viscosity can no longer be neglected; (*b*) the change of the ionic strength could change (*i*) the coupling of the cytoskeleton to the lipid-protein bilayer or (*ii*) the interaction between the highly charged cytoskeletal molecules (Stokke et al., 1986) or (*iii*) the interaction between the hemoglobin and the cytoskeleton; (*c*) the mutual interaction of the cytoskeleton of the opposing membranes. The last possibility is suggested by the finding of Zarda et al. (1977) that the cell thickness in the center is below the limit of resolution and by the elegant experiment of Bull et al. (1986), suggesting that the distance of closest approach of the two opposing membranes is of the order of 600 Å.

Temperature Dependence. The temperature dependence of the shear modulus, μ, is of interest for the following reason. Provided μ was determined by the cytoskeleton and the latter behaves as a typical polymer network, μ should decrease with increasing temperature. For that purpose the deformation amplitude A of a single cell is measured continuously while the temperature is increased (at a rate of 6° per minute) from 5 to 60°C. At 45°C the cell flickering becomes much faster and stronger, which probably indicates the beginning of cytoskeleton denaturing. At $T \approx 50$°C a membrane stiffening sets in. In agreement with Waugh and Evans (cf., Waugh, 1977) the shear modulus

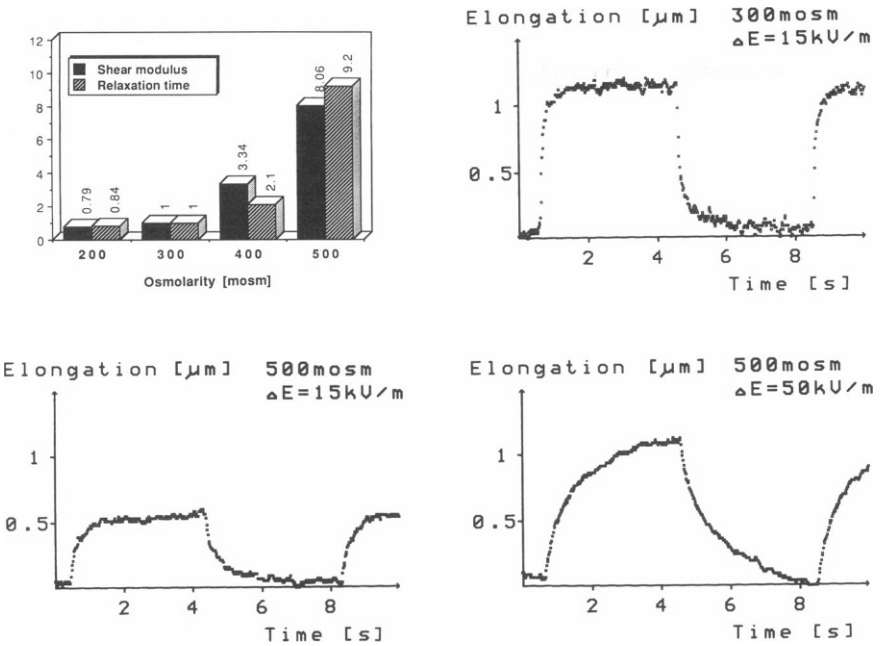

FIGURE 10 Demonstration that a change of the osmolarity beyond the physiological value (300 mosm) has drastic effects on the shear elastic modulus and on the relaxation time, whereas reducing the osmotic pressure hardly changes these values. Probably the assumption that the cytoplasm viscosity is negligible is no more justified for high osmolarities (see text). (*Top left*) Demonstration that a change of osmolarity beyond the physiological value (300 mosm) has a drastic effect on the shear elastic modulus and relaxation time, whereas reducing the osmotic pressure hardly changes these parameters. Note that the values are given relative to the physiological conditions (300 mosm). The numbers of measured cells at 200, 300, 400, 500 mosm are 8, 8, 7, and 4, respectively. (*Top right*) Typical response function under physiological condition. (*Bottom*) Response functions at 500 mosm as obtained at a small (*left*) and a high (*right*) deformation amplitude. The high osmolarity greatly reduces the elongation as compared with *top right*. Comparison of left and right curve shows that the relaxation time increases with increasing amplitude in contrast to the finding at normal pressure (cf., Fig. 3, *bottom*).

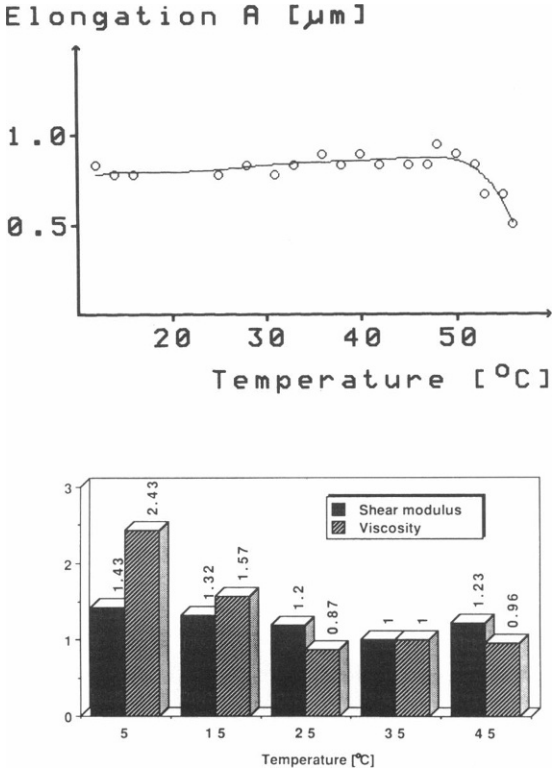

FIGURE 11 Temperature dependence of deformation amplitude as it is typically measured for a single red cell. Field jump experiments (see Fig. 6) are performed while the temperature is scanned from 10 to 60°C. (*Bottom*) Bardiagram of mean values of the shear elastic modulus and membrane viscosity shown for different temperatures. Below 20°C the membrane viscosity strongly increases with decreasing temperature. (Note that the values of μ and η are given relative to those of 35°C. The numbers of measured cells at 5, 15, 25, 35, and 45°C are 16, 7, 12, 17, and 12, respectively).

increases with temperature between 5 and 35°C and thus does not behave as an ideal network of entropy springs as was suggested by Stokke et al. (1986).

The viscosity increases remarkably with decreasing temperature below ~20°C and is essentially constant between 20 and 35°C. The effect is much smaller than the sixfold increase of η between 37 and 6°C reported by Hochmut et al. (1980). The finding that η starts to increase remarkably at $T \leq 20$°C is in agreement with lipid lateral diffusion measurements (Kapitza and Sackmann, 1980) and sedimentation experiments (Glaser and Herrmann, 1980) which indicate the beginning of a phase change (possibly the onset of phase separation) below $T = 20$°C.

Changes of Shear Rigidity Caused by Elliptocytosis

To examine the usefulness of the present technique to detect subtle changes of the membrane structure induced by diseases, elliptic cells from patients suffering from the Leach-phenotype are studied. About 10% of the cells are strongly and 20% weakly elliptic whereas the rest exhibits normal shapes. Fig. 12 summarizes the result. Both the weakly and strongly elliptic cells exhibit a two- to threefold higher shear modulus than cells of normal donors whereas the membrane viscosity is hardly changed. The present result is at variance with the findings of Waugh (1987), who observed a decrease in shear rigidity by the micropipette method. In view of the good agreement of the elastic constants obtained with the two techniques this discrepancy is most probably due to the different defects of the two types of elliptocytosis. In the case of the Leach-phenotype only the sialoglycoproteins, β, β_1, and γ (=gly-

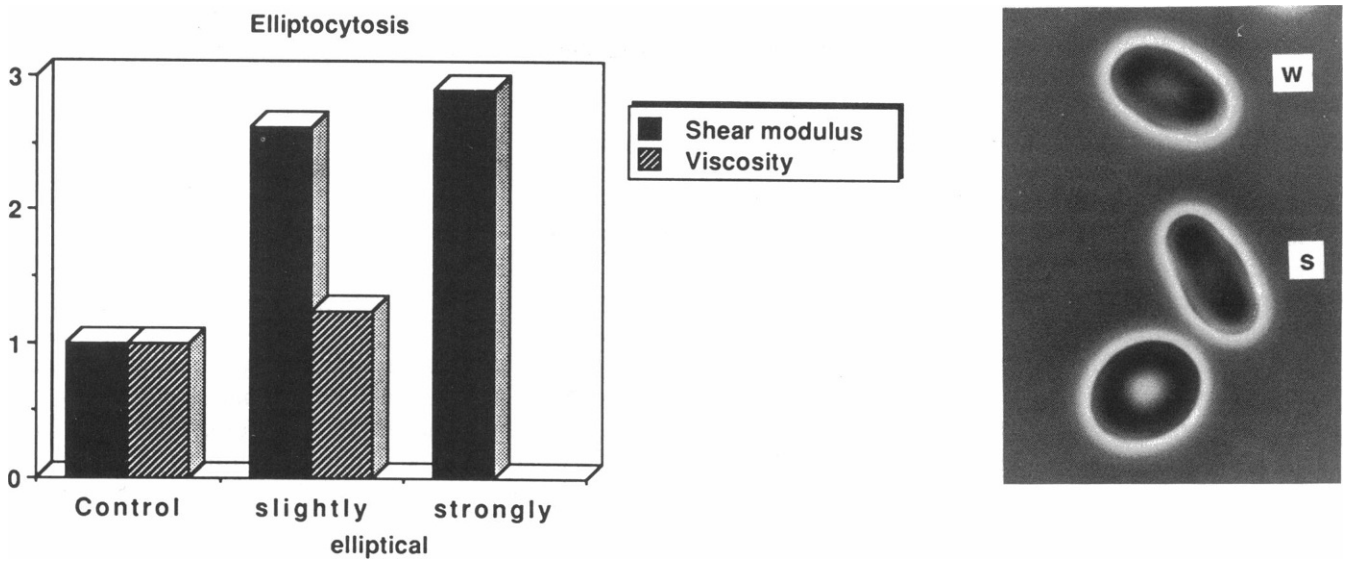

FIGURE 12 Shear rigidity and membrane viscosity of cells from patients suffering from elliptocytosis of the Leach phenotype. Control cells are from normal donors undergoing the same history of bleeding, shipping, and preparation. The micrograph shows a weakly (*w*) and a strongly (*s*) elliptic cell as well as a normal discocyte of the same blood sample. (Note that the values are given relative to the control cells. The numbers of measured cells are 21 control, 23 slightly elliptical, and 5 strongly elliptical.

cophorin C) are missing (Anstee et al., 1984*a* and *b*) whereas the cells studied by Waugh (1987) lack also band 4.1 protein. Because the latter is supposed to play an essential role for the coupling of the spectrin/actin network to the glycophorin (Lux, 1979) the decrease in μ observed by Waugh might be attributed to the weaker coupling of the network to the bilayer as well. In fact antibody mapping studies exhibit 5×10^4 β- and β_1-sialoglycoproteins per cell which is comparable with the number of band 3–ankyrin complexes. The spectrin–band 4–glycophorin interaction could thus provide a similar contribution to the coupling of the network to the membrane as the coupling via the spectrin–ankyrin–band 3 pathway. But why does the absence of β, β_1, and γ alone lead to the observed increase in μ? One possible explanation is that in the absence of these sialoglycoproteins band 4.1 causes stronger cross-linking of spectrin. As will be shown below cross-linking of spectrin indeed increases the shear rigidity strongly.

We also performed preliminary studies of the changes in shear rigidity of cells from patients lacking blood group antigens (Rh_{null}-type stomatocytosis; Kuypers et al., 1984). The cells are cup shaped. The shear modulus of these cells is by about a factor of two smaller than that of normal cells. Because the cytoskeleton is coupled to these receptor proteins, the decrease could again be explained in terms of its decoupling from the lipid/protein bilayer.

Biochemical Modification

As an example of a biochemical modification of the cytoskeleton we cross-linked the spectrin by the bivalent SH-agent diamide following the procedures of Fischer et al. (1978*c*). In addition the reversibility of the effect by the reducing agent DTE (= dithioerythritol which splits S-S bonds) is studied. Before the incubation with diamide (1 mM for 15 min) the cells are treated with iodoacetate to oxydize the intracellular pool of glutathion and avoid desactivation of the diamide.

Fig. 13 shows the effect of diamide incubation on the shear rigidity and on the membrane viscosity in two buffers

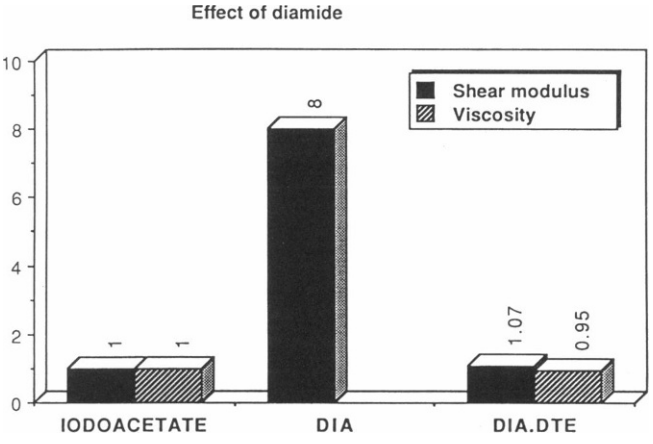

FIGURE 13 Effect of SH-reagent diamide on shear modulus and membrane viscosity and its reversibility after reducing the S-S cross-links with dithioerythritol (DTE). (*First pair of bars*) Values for the cells pretreated with iodoacetate (10 mM, 15 min at 37°C) to inactivate the intracellular glutathione, μ and η arbitrarily set one; (*second bar*) data obtained after treatment with diamide (1 mM, 15 min at 37°C) at an osmotic pressure of 250 mosm; (*third pair of bars*) after treatment of previous sample with DTE (10 mM, 1 h at 37°C). The bar for the viscositie of the diamide-treated cells is missing because the response times are shorter than 20 ms, the resolution limit of our experiment. (Note that the values are given relative to the cells treated with iodoacetate. The numbers of measured cells are 15 iodoacetate, 12 diamide, and 14 diamide-DTE.

of different osmolarity, namely 250 and 600 mosm. The shear modulus is increased by a factor of eight if incubation occurs in the former and by a factor of 50 for incubation in the latter buffer. In contrast the viscosity is only slightly affected. The effect is completely reversible by DTE at 250 mosm but only partially at 600 mosm. Interestingly, the enhancement of the cross-linking effect of diamide by deflating the cell is only observed if the incubation occurs at the high osmolarity, but not if the cell is deflated after completion of the cross-linking reaction.

Another interesting finding is that the cells can only be stretched to a certain extent before buckling sets in. The high sensitivity of diamide-treated cells towards buckling has been reported by Fischer et al. (1981). It suggests that the shear rigidity is much more increased than the bending stiffness. Indeed, separate experiments by the flicker spectroscopy show that the bending modulus is only increased by a factor of two to three after the same diamide treatment (K. Zeman, this laboratory, unpublished results).

The effect of diamide on erythrocytes has been studied carefully by several groups. Kuranstin-Mills and Lessin (1981) demonstrated that it mediates the formation of S-S bonds between spatially adjacent SH groups but is not bound itself. Moreover it does not cross-link hemoglobin or integral membrane proteins but primarily the spectrin. Both inter- and intramolecular S-S bonds are formed: about one per 30 spectrin-dimers of the former and one per three spectrin-dimers of the latter type (Fischer et al., 1978*c*; Haest et al., 1977).

CONCLUDING REMARKS

Reliability of the Technique

The present technique of manipulation of cells in HF electric fields allows precise measurements of the membrane viscoelastic parameters in the linear and nonlinear range of elongation and, as far as the forces involved are concerned, bridges the gap between flicker spectroscopy and the micropipette technique.

A certain drawback of the present method is the rapid aging of the cells in the buffer of low ionic strength, which is necessary to reach the frequency-independent domain of Maxwell-Wagner polarization. This problem is, however, overcome by the fast measuring technique.

The elastic constant μ of an individual cell may be measured with high accuracy ($\pm 4\%$). In contrast, the variability of μ within one cell population is very large: $\pm 45\%$, whereas the scattering of the average μ values of cells of different donors accounts to about half that value ($\pm 18\%$). As noted above, the large variability of the μ and η values of one population is a consequence of the different cell age and can be reduced to some extent by density separation of the cells by centrifugation. Unfortunately the standard deviations of the cells separated by centrifugation are still rather large (Clark et al., 1985).

Thus, whereas it is possible to detect subtle changes of the membrane structure caused during the measurement (for instance by biochemical reactions), it is much more difficult to detect changes in the absolute value of μ or η as caused for instance by diseases. For that purpose a technique allowing the simultaneous measurement of these parameters for many cells would be desirable. Such a technique is presently being developed in our laboratory.

A further important question is whether the evaluation of the deformation in terms of the ellipsoidal model yields reliable absolute values of μ. For a more realistic calculation of the strain-stress relationship, finite element techniques have to be applied. A preliminary calculation has been performed (Engelhardt, 1987) by considering a lens-shaped shell composed of a triangular network of springs. The calculated stretching of the lens (perpendicular to rotational axis) at constant area and volume leads to the same qualitative behavior as the experimentally observed curve (Fig. 3, *top*) or the ellipsoidal model. We thus conclude that the latter is a good approximation.

Nonlinear Effects and Tip Formation

The approximate analysis of the deformation-force relationship of the erythrocyte in terms of a sphere-to-ellipsoid deformation model describes our experimental results in a satisfactory way up to elongations of $A \approx 3$ μm. The initial shape-change at very small electric forces consists in a bulging of the cell center, as becomes clearly visible by bright field microscopy with small bandwidth illumination in the Soret band. The most pronounced deviations from the present simple shell model occurs at elongations > 3 μm, where a tip forms at the end of the cell facing the distant electrode which is, however, completely reversible (cf., Fig. 2). Erythrocytes behave thus completely different from vesicles or vacuoli of plant cells which assume a balloon-like shape up to a threshold voltage above which instability sets in and a tether forms which stretches to the opposite electrode (Engelhardt, 1987). The unique behavior of the red blood cells appears thus to be a consequence of the coupling of the membrane to the cytoskeleton. To see how the present shell model would have to be modified to account for the observed tip formation three possibilities are considered (cf., Fig. 14): (*a*) a homogeneous and constant degree of shearing up to a maximum stretching ratio λ_m, which would correspond to the maximum extension of the polymer network; (*b*) a decrease of shear modulus at low degree of shearing λ following a suggestion by Fischer et al. (1981) which could be of the form

$$\mu = \mu_0 \left(1 + \frac{5}{1 + \exp(100\lambda_0/\lambda)}\right); \qquad (26)$$

and (*c*) dependence of the electric force on curvature.

The first two assumptions lead to a conical shape but cannot generate a tip with a region of negative curvature as found in Fig. 2. The third consideration accounts for the

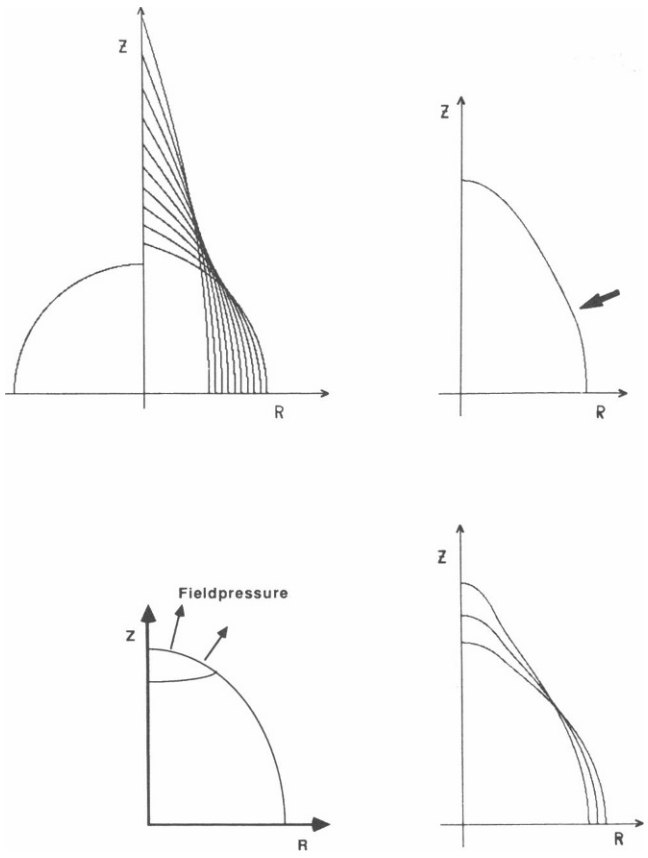

FIGURE 14 This figure shows three different models analyzed to elucidate the origin of tip formation at high electric field strength. Z is the rotational axis. (*Top left*) Shape obtained for a spherical shell deformed under constant area and constant local extension ratio λ. (*Top right*) Shape obtained for a shell with a shear modulus μ which is a function of the extension ratio λ. Here it is assumed that μ increases to a fivefold value if the extension ratio exceeds a certain limit (Fischer, 1981). This leads to a sharp bend (*arrow*) but not to a tip formation. (*Bottom*) Tip formation is observed in a model where the force is acting within a small region only (*bottom left*). It is assumed that there is a positive feedback between the increase of electric field and increasing curvature. Thus the force could dominate at the tip where the curvature is largest.

fact that the force on an ellipsoid is not proportional to $\cos^2\theta$ at large elongation but depends on the curvature, $1/R$, according to $P_{el} \propto R^{-2}$. The force is therefore stronger at the outer end of the ellipsoidal shell. The shape shown in Fig. 14 bottom is obtained by assuming that the electric force acts only in a small region at the outer end of the shell (cf., Fig. 14, *bottom left*).

First of all we are most grateful to E. Evans for many enlightening and helpful discussions and to A. Fischer for introducing us into problems of spectrin crosslinking. The help of H.-P. Duwe with the image processing system is gratefully acknowledged. We are grateful to Dr. Tanner for providing us with cells of patients suffering from elliptocytosis (Leach phenotype) and stomatocytosis (Rh_{null}).

The work was supported by the Deutsche Forschungsgemeinschaft, the Fonds per Chemischen Industrie, and the Leonhard-Lorentz-Stiftung.

Received for publication 4 January 1988 and in final form 12 May 1988.

REFERENCES

Anstee, D. J., S. F. Parsons, K. Ridgwell, M. J. A. Tanner, A. H. Merry, E. E. Thomson, P. A. Judson, P. Johnson S, Bates, and I. D. Fraser. 1984*a*. Two individuals with elliptocytic red cells apparently lack three minor erythrocyte membrane sialoglycoproteins. *Biochem. J.* 218:615–619.

Anstee, D. J., K. Ridgwell, M. J. A. Tanner, G. L. Daniels, and S. F. Parsons. 1984*b*. Individuals lacking the gerbich blood-group antigen have alterations in the human erythrocyte membrane sialoglycoproteins β and γ. *Biochem. J.* 221:97–104.

Bessis, M., and N. Mohandas. 1975. A diffractometric method for the measurement of cellular deformability. *Blood Cells (Berl.).* 1:307–313.

Brochard, F., and J. F. Lennon. 1975. Frequency spectrum of the flicker phenomenon in erythrocytes. *J. Physique.* 11:1035–1047.

Bryant, G., and J. Wolfe. 1987. Electromechanical stresses produced in the plasma membranes of suspended cells by applied electric fields. *J. Membr. Biol.* 96:129–139.

Bull, B. S., R. S. Weinstein, and R. A. Korpman. 1986. On the thickness of the red cell membrane skeleton: quantitative electron microscopy of maximally narrowed isthmus regions of intact cells. *Blood Cells (Berl.).* 12:25–42.

Clark, M. R., and S. B. Shohet. 1985. Red Cell Senescence. The Red Blood Cell Membrane. *Clin. Haematol.* 14:223–257.

Engelhardt, H. 1987. Manipulation einzelner Zellen mit Hochfrequenzfeldern: eine empfindliche Methode zur Messung viskoelastischer Parameter und zum Nachweis subtiler struktureller Aenderungen der Plasmamembran von Erythrozyten. Ph.D. thesis. Technical University Munich.

Engelhardt, H., H. Gaub, and E. Sackmann. 1984. Viscoelastic properties of erythrocyte membranes in high-frequency electric fields. *Nature (Lond.).* 307:378–380.

Evans, E. A. 1983. Bending elastic modulus of red blood cell membrane derived from buckling instability in micropipet aspiration tests. *Biophys. J.* 43:27–30.

Evans, E. A., and R. Skalak. 1980. Mechanics and thermodynamics of biomembranes. CRC-Press, Boca Raton, FL.

Fischer, T. M., M. Stoehr-Liesen, and H. Schmid-Schoenbein. 1978*a*. The red cells as a fluid droplet: tank tread-like motion of the human erythrocyte membrane in shear flow. *Science (Wash. DC).* 202:894–896.

Fischer, T. M., M. Stoehr, and H. Schmid-Schoenbein. 1978*b*. Red blood cell (RBC) microrheology: comparison of the behavior of single RBC and liquid droplets in shear flow. *AIChE Symp.* 182:38–45.

Fischer, T. M., C. W. M. Haest, M. Stoehr, D. Kamp, and B. Deuticke. 1978*c*. Selective alterations of erythrocyte deformability by SH-reagents. Evidence for an involvement of spectrin in membrane shear elasticity. *Biochim. Biophys. Acta.* 510:270–282.

Fischer, T. M., C. W. M. Haest, M. Stoehr-Liesen, H. Schmid-Schoenbein, and R. Skalak. 1981. The stress-free shape of the red blood cell. *Biophys. J.* 34:409–422.

Flanders, H. 1984. Scientific Pascal. Reston Publishing Co. Inc., Reston, VA.

Flügge, W. 1973. Stresses in Shells. Springer-Verlag, Berlin.

Fricke, K., and E. Sackmann. 1984. Variation of frequency spectrum of the spectrum of erythrocyte flickering caused by aging, osmolarity, temperature and pathological changes. *Biophys. Biochim. Acta.* 803:145–152.

Fricke, K., K. Wirthensohn, R. Laxhuber, and E. Sackmann. 1986. Flicker spectroscopy of erythrocytes. *Eur. Biophys. J.* 14:67–81.

Glaser, R., and A. Herrmann. 1980. The sedimentation of individual human erythrocytes as a function of temperature. *Biorheology.* 17:289–291.

Haest, C. W. M., D. Kamp, G. Plasa, and B. Deuticke. 1977. Intra- and intermolecular cross-linking of membrane proteins in intact erythrocytes and ghosts by SH-oxidizing agents. *Biochim. Biophys. Acta.* 469:226–230.

Hochmut, R. M., P. R. Worthy, and E. A. Evans. 1979. Red cell extensional recovery and the determination of membrane viscosity. *Biophys. J.* 26:101–114.

Hochmut, R. M., K. L. Buxbaum, and E. A. Evans. 1980. Temperature dependence of the viscoelastic recovery of red cell membrane. *Biophys. J.* 29:177–182.

Kapitza, H.-G., and E. Sackmann. 1980. Local measurement of lateral motion in erythrocyte membranes by photobleaching technique. *Biochim. Biophys. Acta.* 595:56–64.

Kurantsin-Mills, J., and L. Lessin. 1981. Aggregation of intramembrane particles in erythrocyte membranes treated with diamide. *Biochim. Biophys. Acta.* 641:129–137.

Kuypers, F. A., M. van Linde-Sibenius-Trip, B. Roelofsen, M. J. A. Tanner, D. J. Anstee, and J. A. F. Op Den Kamp. 1984. Rh_{null} human erythrocytes have abnormal membrane phospholipid organization. *Biochem. J.* 221:931–934.

Landau, L. D., and E. M. Lifschitz. 1959. Course of Theoretical Physics. Vol. 7. Theory of Elasticity. Pergamon Press, London.

Landau, L. D., and E. M. Lifschitz. 1960. Course of Theoretical Physics. Vol. 8. Electrodynamics of continuous media. Pergamon Press, London.

Lux, S. E. 1979. Spectrin-actin membrane skeleton of normal and abnormal red blood cells. *Semin. Haematol.* 16:21–50.

Marquardt, D. W. 1963. An algorithm for least square estimation of nonlinear parameters. *J. Soc. Industrial Appl. Math.* 11:431–441.

Nash, G. B., and H. J. Meiselmann. 1975. Red cell and ghost viscoelasticity effects of hemoglobin concentration and in vivo aging. *Biophys. J.* 42:63–73.

Petersen, N. O., W. B. McConnaughey, and E. L. Elson. 1982. Dependence of locally measured cellular deformability on position on the cell, temperature, and cytochalasin B. *Proc. Natl. Acad. Sci. USA.* 79:5327–5331.

Pfafferot, C., G. B. Nash, and H. J. Meiselmann. 1985. Red cell deformation in shear flow: effects of internal and external phasevelocity and of in vivo aging. *Biophys. J.* 47:695–704.

Pohl, A. H. 1978. Dielectrophoresis. Cambridge University Press, Cambridge.

Sackmann, E., J. Engelhardt, K. Fricke, and H. Gaub. 1984. On dynamic molecular and elastic properties of lipid bilayers and biological membranes. *Colloids Surf.* 10:321–335.

Saito, M., H. P. Schwan, and G. Schwarz. 1966. Response of nonspherical biological particles to alternating electric fields. *Biophys. J.* 6:313–327.

Sauer, F. 1983. Forces on suspended particles in the electromagnetic field. *In* Coherent Excitations in Biological Systems. H. Fröhlich and F. Kremer, editors. Springer-Verlag, Berlin.

Sauer, F. 1985. Interaction-forces between microscopic particles in an external electromagnetic field. *In* Interactions between Electromagnetic Fields and Cells. A. Chiabrera, C. Nicolini, and H. P. Schwan, editors. Plenum Press, New York. 181–202.

Schwan, H. P. 1985. Dielectric properties of cells and tissues. *In* Interactions between Electromagnetic Fields and Cells. A. Chiabrera, C. Nicolini, and H. P. Schwan, editors. Plenum Press, New York. 181–202.

Stokke, B. T., A. Mikkelsen, and A. Elgsaeter. 1986. Spectrin, human erythrocyte shapes, and mechanochemical properties. *Biophys. J.* 49:319–327.

Waugh, R. E. 1977. The temperature dependence of the elastic properties of the red blood cell membrane. Ph.D. thesis. Duke University, Durham, NC.

Waugh, R. E. 1987. Effects of inherited membrane abnormalities on the viscoelastic properties of erythrocyte membrane. *Biophys. J.* 51:363–369.

Zarda, P. R., S. Chien, and R. Skalak. 1977. Elastic deformations of red blood cells. *J. Biomech.* 10:211–221.

Zilker, A., H. Engelhardt, and E. Sackmann. 1987. Dynamic reflection interference contrast microscopy: a new method to study surface excitations of cells and to measure membrane bending elastic moduli. *J. Physique.* 48:2139–2151.

Zimmermann, U., J. Vienken, and G. Piwlat. 1981. Rotation of cells in an alternating electric field. *Z. Naturforsch.* 36:173–177.